Development of New Concepts for the Control of Polymerization Processes: Multiobjective Optimization and Decision Engineering. I. Application to Emulsion Homopolymerization of Styrene

Silvère Massebeuf, Christian Fonteix, Sandrine Hoppe, Fernand Pla

Laboratoire des Sciences du Génie Chimique, UPR CNRS 6811, Ecole Nationale Supérieure des Industries Chimiques—INPL, 1 rue Grandville, BP 451, 54001 Nancy Cedex, France

Received 19 February 2002; accepted 11 September 2002

ABSTRACT: This article deals with the development of a multicriteria analysis, and its application to the optimization of batch emulsion polymerization processes. This new approach in the domain of polymer reaction engineering illustrates how a multiobjective optimization aided by a genetic algorithm and using the Pareto concept of domination is useful. In this process (emulsion homopolymerization of styrene), several objectives were simultaneously required, e.g., a high quality of the resulting products together with a high productivity. The aim of this study was to find the optimal experimental conditions to obtain simultaneously the minimum reaction time and designed values for both average molecular weights and particles size. To do that, an adapted mathematical model, able to describe all the process physicochemical phenomena, was been first elaborated. The multicriteria analysis then gave a set of nondominated points with conflicting criteria. A decision support system was then developed and applied to rank the Pareto solutions set and to propose some good solutions by taking into account the decision maker's preferences. © 2003 Wiley Periodicals, Inc. J Appl Polym Sci 87: 2383–2396, 2003

Key words: emulsion polymerization; modeling; polystyrene

INTRODUCTION

Most real-world problems require simultaneous optimization of multiple objectives. This problem differs from single objective optimization. A set of solutions is obtained, which are not necessarily the optimal solutions if each objective is considered individually. So, the optimization of several conflicting criteria leads to trade-offs solutions, which form the so-called Pareto set or the nondominated solutions set. The Pareto domination can be defined if a potential solution is better than another for all criteria and strictly better for at least one.[1] In polymer reaction engineering, the quality of the products such as the productivity has to be optimized. The operating variables for polymerization reactors influence the properties of the product in conflicting ways. So, a multiobjective optimization approach seems to be adapted to obtain appropriate operating conditions. A recent review on applications of multiobjective optimization in chemical engineering presents several studies on the multiobjective optimization of polymerization reactors.[2] Several recent studies deal with this problem, e.g., an industrial nylon 6 semibatch reactor, a free radical bulk polymerization reactor of methyl methacrylate and an industrial wiped film poly(ethylene terephthalate) reactor.[3–6] Moreover, a genetic algorithm, an artificial intelligence based technique, is used for experimental on-line control.[7,8] Nevertheless, none of these concepts has been applied in emulsion polymerization processes.

The aim of this article is to propose a new multicriteria assistance, multiobjective optimization and decision support system, to the emulsion polymerization of styrene carried out under batch conditions. This process is considered well known. An important criterion for this system is the minimization of the reaction time to achieve a desired final conversion. Other objective functions can be the minimization of the polydispersity index and the attainment of a designed value of the mean particle diameter. The achievement of these properties must lead to desired end-use properties while a high productivity must be kept. Several variables, like initial conditions and composition of the products, can be manipulated to respect an optimal multicriteria set. So, this optimization approach needs a model elaboration to predict all these characteristics. Building a model dedicated to optimization is certainly the nerve center of the approach because, whatever the optimization procedure, it needs evaluation functions determined by a model unit. A num-

Correspondence to: F. Pla (fernand.pla@ensic.inpl-nancy.fr).

Journal of Applied Polymer Science, Vol. 87, 2383–2396 (2003)

ber of studies have given model equations for emulsion polymerization processes to describe polymer features very precisely.[9] In an optimization loop, some hypotheses, which must be justified, are taken into account to simplify the model and reduce the calculus time. So, the aim is to elaborate a tendency model that can be used in a large domain.

This work thus consists in elaborating a simple model of emulsion polymerization of styrene based on a kinetic scheme and in finding the best operating conditions depending on the hypotheses. The multiobjective optimization leads to a trade-off zone and a decision support system allows us to propose some choices by a total ranking of possible solutions.

EXPERIMENTAL

Materials

The chemicals required to carry out the emulsion polymerization are styrene (STY), deionized water, sodium dodecyl sulfate (SDS) as emulsifier, potassium persulfate (KPS) as initiator soluble in water, and hydroquinone to quench the polymerization reaction in withdrawn samples. The monomer was previously distilled under reduced pressure before use, and all other ingredients were used as received.

Polymerization process

The reactor used is schematically described in Figure 1. It is a 1 L jacketed glass batch reactor equipped with a stirrer, a reflux condenser, a cryostat, and an inlet system for nitrogen. The mixer system used is composed of a propeller and an impeller. Its rotation speed is kept constant at 200 rpm.

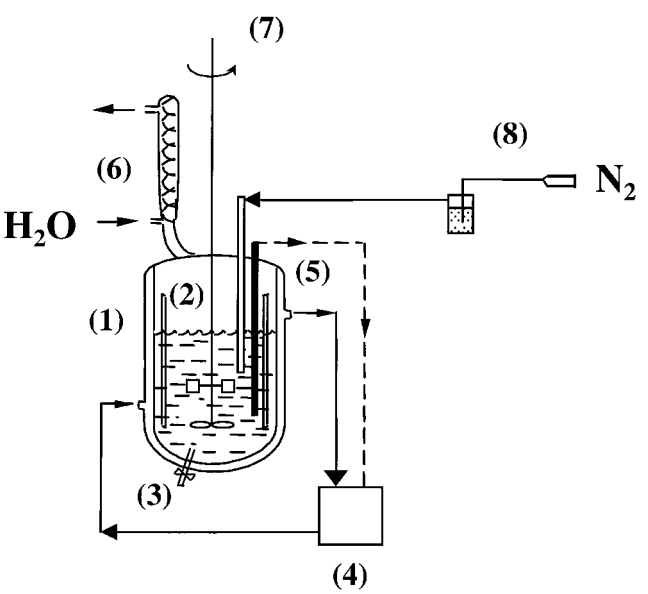

Figure 1 Schematic diagram of the batch reactor used: (1) 1 L jacketed glass reactor; (2) baffles; (3) sample inlet; (4) cryostat; (5) Pt 100 probe; (6) reflux condenser; (7) stirrer; (8) inlet system for nitrogen.

TABLE I
Typical Recipe for the Batch Emulsion Polymerization of Styrene

	Reagent	Weight (g)
Reactor charge	H_2O	780
	STY	200
	SDS	5
Initiator solution	H_2O	20
	KPS	1

A typical recipe is shown in Table I. For all experiments, the polymerizations were carried out at 60°C with 200 g of styrene and 800 g of water. The corresponding weights of SDS and KPS were chosen between 1 and 7 g and 0.2–1 g, respectively.

The reactor vessel was charged with the desired amount of water, monomer, and surfactant, which form after mixing an emulsion. The batch was heated and the reaction mixture was purged by bubbling nitrogen for about 20 min. The initiator was then added, the polymerization began and the reactor temperature was controlled by circulating water through the reactor jacket via the thermostatic bath. Samples were collected from the reactor at appropriate time intervals to measure the characteristics of the resulting polymer.

Characterization of lattices and macromolecules

In order to follow the emulsion polymerization, analytical methods have been developed to get experimental data. During the polymerization, samples were taken in glass vessels containing small amount of hydroquinone to stop reaction. The resulting products were then characterized by chemical and physical analysis.

Monomer conversion

The monomer conversion was determined gravimetrically using a Mettler HG 53 thermoscales. About 1 g of latex was placed on an aluminum plate, which was introduced in the thermoscales and heated to 175°C to evaporate completely water and residual monomer. The mass of the final dried sample, which corresponds to the mass of polymer, surfactant, and initiator, was automatically measured. After correction of the remaining amounts of initiator and surfactant, according to the knowledge of their mass introduced in the reactor, the monomer conversion was determined.

TABLE II
Kinetic Scheme for Emulsion Polymerization of Styrene

Initiation	$I \xrightarrow{fk_d} 2\,R_w$
Nucleation	$R_w \xrightarrow{k_{cm}} R_0$
Propagation (in the particles)	$R_x + M \xrightarrow{k_p} R_{x+1}$
Chain transfer to monomer (in the particles)	$R_x + M \xrightarrow{k_{trM}} P_x + R_0$
Capture by particles	$R_w \xrightarrow{k_{cp}} R_0$
Instantaneous termination (in the particles)	$R_x + R_0 \rightarrow P_{x+1}$

Average particle size

The average particle size was determined by use of a Malvern 4700 quasi-elastic light scattering apparatus. After dilution of the samples with deionized water, the unswollen average particle diameter was measured. This value, together with that of the overall conversion, was then used to estimate the number of polymer particles per liter of latex.

Number and weight average molecular weights

The number and weight average molecular weights were determined by size exclusion chromatography (SEC) using a double detection: a multiangle laser light scattering (MALLS) apparatus (Dawn DSP-F) and a differential refractometer (Waters 410, Millipore). Elutions were performed at 35°C with tetrahydrofuran (THF) containing di-tertiary-butyl-2.6 methyl-4 phenol as stabilizer. The flow rate was 1 mL/min. The concentration of the polymer solutions and the corresponding injected volume were 1 g/L and 25 μL, respectively,. Prior to chromatography, THF and polymer solutions were passed through a Nylon filter of 0.45 μm porosity. The SEC assembly consisted of a degasser, a Waters 510, Millipore pump, a U6K, Millipore injector, a precolumn, two chromatographic columns assembled in series and filled with linear ultrastyragel, and an electric oven to control the temperature of the columns. Data from the two detectors were acquired and computed by use of the software Astra from Wyatt Technology, which allowed us to determine the molecular weight distribution and the number and weight average molecular weights of the samples.

THEORY

In this section, three theoretical aspects are developed. They concern (1) the elaboration of the model describing the polymerization process, (2) the basis of the multicriteria optimization, and (3) the concepts governing the decision aid.

Mathematical model

Developing an optimization procedure needs a mathematical model to describe polymer features. The aim is to elaborate a model with assumptions allowing us to simplify the whole system. The approach consists (1) in expressing hypotheses on mechanisms and physicochemical phenomena, (2) in writing mass balances deduced from these assumptions, and (3) in developing submodels to estimate some properties of the polymer. Finally, the determination of the model parameters, from the experimental data available, allows us to present results of the simulator.

Kinetic scheme

Writing the kinetic mechanism, which takes into account all the basic assumptions concerning the process, is the crucial step. This gives rise to mass balances of all components in the reactor. In order to write the model equations, the following assumptions are made:

1. Due to the hydrophobic character of the styrene (water solubility: 4×10^{-3} mol/L at 50°C), propagation, chain transfer to monomer, and termination reactions in the aqueous phase, as well as radical desorption from the particles, are neglected.
2. Termination reactions in the particles are considered to be very fast as compared to the radical entry into the particles; thus it is assumed that there is no more than one radical per polymer particle (zero-one system).[10] The termination reactions are then possible by chain transfer to monomer and by capture of a new radical by the particle. This assumption is generally expressed for the emulsion homopolymerization of styrene. This leads to consider the termination rate constant as an infinitive coefficient. The literature confirms this assumption: $k_t = 10^4$ to 10^{11} L/mol s at 60°C, depending on the authors.[11] So, this parameter is a few sensitive one in the whole system.
3. The reactor is perfectly mixed and isotherm.
4. There is no coagulation between particles.

Table II shows a classical kinetic scheme for the emulsion polymerization of styrene where w represents the water phase and x the degree of polymerization.

Kinetic reaction rates

From the kinetic scheme given in Table II, rate expressions can be calculated for a batch system in moles per volume and time unit. The initiator decomposition rate is

$$R_d = k_d I_w \tag{1}$$

where k_d and I_w are the initiator decomposition rate constant and concentration in the aqueous phase, respectively.

The propagation and transfer to monomer reaction rates are

$$R_p = k_p[M]_p \frac{N_p \bar{n}}{\mathcal{N}_A} \tag{2}$$

$$R_{trM} = k_{trM}[M]_p \frac{N_p \bar{n}}{\mathcal{N}_A} \tag{3}$$

where k_p and k_{trM} are the propagation and the transfer to monomer reaction rate constants respectively, $[M]_p$ is the monomer concentration in the polymer particles, N_p is the particle number per volume unit, $\bar{n}$ is the average number of radicals per particle, and $\mathcal{N}_A$ is Avogadro's number.

The termination reaction rate is considered as instantaneous in the particular case of the zero-one model adopted in this system. So, the termination reaction rates is limited by radical capture for particles that contain one radical yet.

Nucleation

The nucleation remains today an important subject of discussion. This operation must be known in order to predict the number of particles vs initiator, surfactant and monomer concentrations. Moreover, the partition of the different components between each phase (water, monomer droplets, particles, and micelles) must be determined because of the heterogeneity of the emulsion polymerization system. Two mechanisms are generally proposed, micellar and homogeneous nucleation, but other approaches have also been considered.

When the surfactant concentration is higher than the critical micellar concentration (CMC), radicals generated by initiator decomposition are caught by monomer-swollen micelles.[12] Particles are then created. A portion of the micelles is used for nucleation and the rest allows us to stabilize the particles. Nucleation is stopped when all micelles are consumed. Then, the particle number generally becomes constant. An expression has been proposed by Smith and Ewart[13] giving the particles number vs surfactant and initiator concentration: $N_p \propto [S]^{0.6}[A]^{0.4}$. This theory has been generalized by Gardon,[14] but the main problem is that micellar nucleation is not appropriate when the surfactant concentration is lower than the CMC.

Homogeneous nucleation has been elaborated to overcome limitations of the micellar nucleation theory. Oligoradicals can propagate in the aqueous phase until a critical chain length, before coagulation and formation of particles.[15] The particle number depends on initiator decomposition, on the capture of the resulting radical, and on eventual coagulation. A complete model has been developed to describe all these phenomena.[16]

The two nucleation theories are commonly used even if a measure of the particle size distribution, at the end of nucleation, shows that nucleation cannot be considered in a one-step process.[17] Moreover, the use of a water-insoluble dye allows us to probe the particle nucleation loci in styrene emulsion polymerization.[18] Most of the dye molecules are present in monomer droplets and in the micelles. The mixed modes of particle nucleation (homogeneous and micellar) can be then proposed with the determination of the amount of dye incorporated into the resulting latex particles.

The two nucleation theories are considered in our system, according to surfactant amount available in the aqueous phase. Three elements have to be taken into account in the model: the radicals, the monomer, and the surfactant. If one is not present, nucleation is not possible. Surfactant balance is

$$S_0 = S_p + S_m + S_w + S_g \tag{4}$$

where S_0, S_p, S_m, S_w, and S_g are the initial concentration of surfactant and the concentrations of the surfactant adsorbed on the particles, on the micelles, soluble in water, and adsorbed on the droplets respectively. S_p can be expressed as

$$S_p = \frac{A_p}{a_s} \tag{5}$$

where A_p is the particles surface area per volume unit and a_s the surface area of 1 g of surfactant. In the following, S_g is neglected because droplets represent a small surface area compared to the micelle one.

If the initial concentration of surfactant is lower than the CMC, no micelle is formed and the nucleation is homogeneous. In the opposite case, micelles are formed and the aqueous phase is saturated by the surfactant. This leads to the following mathematical equations:

$$\text{If } S_{cmc} + \frac{A_p}{a_s} < S_0, \text{ micelles can be formed.}$$

$$\text{Then} \begin{cases} S_m = S_0 - S_{cmc} - \dfrac{A_p}{a_s} \\ S_w = S_{cmc} \end{cases}$$

$$\text{Else} \begin{cases} S_m = 0 \\ S_w = \max\left(S_0 - \dfrac{A_p}{a_s}, 0\right) \end{cases} \tag{6}$$

where S_{cmc} is the critical micellar concentration.

Then, the nucleation rate can be written as the sum of micellar and homogeneous nucleation rates:

$$R_{cm} = R_{cmm} + R_{cmh} = k_{cm}[R_w](S_m + (S_w - S_e)) \quad (7)$$

where k_{cm} is a proportionality coefficient. This equation indicates that the micellar nucleation rate, R_{cmm}, is proportional to the radical concentration in the aqueous phase, $[R_w]$, and to the surfactant concentration in the micelles potentially formed S_m. Simultaneously, it shows that the homogeneous nucleation rate is proportional to the radical concentration in the aqueous phase, $[R_w]$, and to the "efficient" surfactant concentration in the aqueous phase $(S_w - S_e)$. The introduction of this efficient concentration is due to the observed phenomenon. If too few amount of surfactant is present in the reactor, no nucleation is taken into account. Then, below a given limited concentration S_e, it is impossible to create particles.

Rate of entry of radicals into particles

The capture corresponds to the adsorption of a radical by a particle. If the particle contains one radical yet, a termination reaction is instantaneously considered. If the particle does not contain any radical, propagation can take place. Several theories can be mentioned to express the capture rate. First of all, the diffusion theory allows us to write that the capture rate is proportional to the radius of swollen particles.[19] No radical concentration gradient has been considered, in a second theory, so that collision between radicals and particles allows us to consider the capture rate as proportional to the square of the particle radius.[20] A third theory has been proposed: radical entry is treated like a production flow in the particles, which depends on the particle volume.[21]

We have chosen to consider that the capture rate is proportional to the average diameter of the swollen particle, $\bar{d}_p$. The capture rate is then expressed as a function of both number of particles Np and free radicals concentration in the aqueous phase $[R_w]$:

$$R_{cp} = k_{cp}\bar{d}_p \frac{N_p[R_w]}{\mathcal{N}_A} \quad (8)$$

where k_{cp} is the capture rate coefficient.

Mass balances

From the kinetic scheme and the rate expressions of each elementary reactions, mass balances of each component can be written. Two main components are in the aqueous phase: the initiator and radicals resulting from its thermal decomposition. This decomposition gives

$$\frac{dI_w}{dt} = -k_d I_w \quad (9)$$

The corresponding efficient free radicals are formed by initiator decomposition and can be captured by micelles and particles:

$$\frac{dR_w}{dt} = 2fk_d I_w - R_{cm} - R_{cp} \quad (10)$$

where f is the radical efficiency. The quasi-steady-state approximation is usually used to determine the initiator radical concentration in the water phase,[13] but eq. (10) can also be written like that in the whole differential equations system.

The monomer is consumed by propagation and chain transfer to monomer reactions:

$$\frac{dM}{dt} = -R_p - R_{trM} \quad (11)$$

The corresponding conversion rate expression $[X = (M_0 - M)/M_0]$ is then deduced, where M_0 is the initial monomer concentration:

$$\frac{dX}{dt} = \frac{R_p + R_{trM}}{M_0} \quad (12)$$

Particle number

The particles are created by nucleation:

$$\frac{dN_p/\mathcal{N}_a}{dt} = R_{cm} \quad (13)$$

With the zero-one assumption, it is quite easy to determine the number of radicals per particle $\bar{n}$. An approximation is to directly consider $\bar{n} = 0.5$ or to write the balance of the particle containing 1 radical:

$$\frac{dN_p\bar{n}/\mathcal{N}_a}{dt} = R_{cm} + R_{cp}(1 - \bar{n}) - R_{cp}\bar{n} \quad (14)$$

This balance allows us to reach $\bar{n}$, which was an unknown term in eqs. (2) and (3).

Molecular weight distribution (MWD)

The molecular weight distribution gives information that expresses all chemical and physical processes to form macromolecules. The molecular weight measurements concern macromolecules and macroradicals be-

cause the reaction is stopped by addition of hydroquinone. The molecular weights are measured from the dead chains in the sample, which correspond to active and dead chains during the reaction. The determination of the distribution moments was inspired by Villermaux and Blavier, who developed a method for modeling free radical homogeneous polymerization reactions.[22] This moments method is adapted here to determine the moments of the molecular weight distribution in emulsion polymerization.

In the case of the macroradicals, the number of active chains corresponds to $N_p\bar{n}$. The mass balance of the average kinetic chain length, $\bar{\lambda}$ is then deduced:

$$\frac{d(N_p\bar{n}\cdot\bar{\lambda})/\mathcal{N}_a}{dt} = R_p - (R_{cp}\bar{n} + R_{trM})\bar{\lambda} \qquad (15)$$

The $\bar{\lambda}$ is modified by both propagation and chain termination reactions, i.e., chain transfer to monomer reactions and capture in the zero-one model. This simple balance is written assuming that the distributions of both the number of radicals per particle and the degree of polymerization of active chains are considered independent. This hypothesis is admissible for the zero-one system.

The balances of the moments can be expressed, for a number of chains N_c as

$$\frac{dN_c/\mathcal{N}_a}{dt} = R_{cm} + R_{trM} + R_{cp}(1-\bar{n}) \qquad (16)$$

$$\frac{d(N_c\lambda)/\mathcal{N}_a}{dt} = R_p + R_{cp}\bar{n} \qquad (17)$$

$$\frac{d(N_c\lambda_2)/\mathcal{N}_a}{dt} = (R_p + R_{cp}\bar{n})(1+2\bar{\lambda}) \qquad (18)$$

where λ and λ_2 are the average and the second moment of the degree of polymerization, respectively.

Multicriteria optimization

General considerations

Every day we are confronted with multiobjective decision in real-world problems. In particular, in manufacturing processes, production, costs, and product quality have to be optimized simultaneously. All these objectives are rarely optimal for the same experimental conditions. In chemical engineering, multiple objectives have usually been combined, through linear combination to form a scalar objective function.[23] This technique depends on the user's preconceptions so that preferences can bias the results and a large number of single objective optimization runs have to be executed to obtain different optimal points. So, simultaneous optimization of conflicting attributes leads us to obtain a set of solutions that are superior to the rest of the solutions in the search space. Methods incorporating a domination criterion allow us to find a zone, called the Pareto domain, defined by the set of all nondominated points. For the Pareto domination criterion, a point dominates another if it is strictly better for at least one criterion, and better or equal for the others. Consequently, evolutionary algorithms are well-suited to multiobjective optimization to keep a set of points along the Pareto trade-off region.[24]

A multicriteria optimization method has been developed and applied to emulsion polymerization of styrene. The criteria are defined from the model that has been elaborated. The aim is now to simultaneously obtain several polymer properties. So, the model has to be fitted in with the multicriteria optimization procedure.

Algorithmic development

Considering that evolutionary algorithms are well suited to multiobjective problems, our approach used a diploid genetic algorithm whose principles were previously elaborated.[25,26] The aim of this section is to adapt the diploid genetic algorithm to the multicriteria case. A set of m given points is randomly generated. All individuals are evaluated by the calculation of each objective f_i ($i = 1, \ldots, n$). Then, to each point x_j, is associated a value, $F(x_j)$, which corresponds to the number of times that this point is dominated by all the others in the current generation:

$$F(x_j) = \sum_{p=1}^{m} h_{jp} \text{ where } \begin{cases} h_{jp} = 1 & \text{if } x_p \text{ dominates } x_j \\ h_{jp} = 0 & \text{else} \end{cases} \qquad (19)$$

Let be denoted by n, the number of criteria. For two points x_j and x_p of the same population, and for all criteria i ($i = 1, \ldots, n$):

$$\begin{aligned} &\text{if } f_i(x_j) \text{ is WORSE THAN } f_i(x_p): && c_{ijp} = 0 \\ &\text{if } f_i(x_j) \text{ is BETTER THAN } f_i(x_p): && c_{ijp} = n+1 \\ &\text{if } f_i(x_j) \text{ is EQUAL TO } f_i(x_p): && c_{ijp} = 1 \end{aligned} \qquad (20)$$

where c_{ijp} is an intermediate variable.

In the case of minimization, WORSE THAN is equivalent to $<$, and BETTER THAN is equivalent to $>$.

$$\text{if } \sum_{i=1}^{n} c_{ijp} < n, \text{ then } h_{jp} = 1 \text{ and } h_{pj} = 0 \text{ because } x_j \text{is dominated by } x_p$$

TABLE III
Classified Individuals in the *k*th Generation

X	x_1	x_2	x_3	$\cdots$	x_s	x_{s+1}	$\cdots$	x_t	x_{t+1}	$\cdots$	x_m
F	0	0	0	$\cdots$	0	$F(x_{s+1})$	$\cdots$	$F(x_t)$	$F(x_{t+1})$	$\cdots$	$F(x_m)$

$$\text{if } \sum_{i=1}^{n} c_{ijp} \geq n \text{ and } \sum_{i=1}^{n} c_{ipj} \geq n, \text{ then } h_{jp} = h_{pj} = 0 \ (h_{jj} = 0) \tag{21}$$

So, for each point, a value F corresponds by applying the Pareto domination criterion. Then, all the points may be classified. The value of the function for the better individuals in the current generation is equal to zero. The classified individuals and their function value are presented in Table III in the kth generation.

Let be denoted s, the better individuals that are nondominated in the current population (k) and are the chosen parents for the next ($k + 1$). The ($m - s$) worse individuals are eliminated for the next generation but are used for the children evaluation. Each new individual is compared with all m points in the previous population. Then, a threshold t is defined to keep the best children:

$$t = s + E[p_t(m - s)] \tag{22}$$

where $E[x]$ is the entire part of x and p_t is a parameter empirically chosen (e.g., 0.3). So, a child death rate is applied to the convergence when the new individual x_j is worse than the individual x_t, i.e., $F(x_j) > F(x_t)$. When the new population is reformed, all m points are evaluated with the new values of function F. The population of each generation is evaluated until the stopping criterion is satisfied: all the points are nondominated—that is to say, that F is equal to zero for the m points.

Decision aid

Many authors who use evolutionary algorithms to multiobjective optimization often give a good approximation of the Pareto zone. However, in chemical engineering, the industrialist does not want an optimal zone but the best solution. So, after the Pareto set has been obtained, we are confronted by a multiple-criteria decision problem to classify all nondominated points. Then, the decision maker has to define his/her preferences based on his/her knowledge of the process. These expressions allow us to propose a decision support system that aggregates all the decision maker's preferences.

Generally, in chemical engineering, system responses have a physical interpretation. For this study, we have chosen to use a partial aggregation for modeling the preferences.[27] All nondominated solutions can be compared two by two to show a possible outranking before a total synthesis of the alternatives. A type ELECTRE structure seems to be the most appropriate method for the process control problem and with the knowledge of the criteria values.[28]

Decision support system shell

A multicriterion analysis algorithm has been developed with a comparison process between alternatives two by two. The decision maker has to express several parameters to define his/her preferences. He/She must introduce the weights w_k of each criterion k, depending on the relative importance of the criteria. In the algorithm, these coefficients have been normalized:

$$\sum_{k=1}^{n} w_k = 1 \tag{23}$$

Moreover, the decision maker has to define indifference q_k, preference p_k, and veto v_k thresholds for each criterion. The indifference threshold is defined so that two points cannot be differentiated below this threshold. The preference threshold is defined to show the real preference of one alternative against another. And the veto threshold is defined like a constraint if an alternative is too bad in one criterion. A point will be penalized if one of its criteria is over the veto threshold compared to another point, even if it is considered a good point for the other criteria. So, the three thresholds are defined for each criterion in such a way that

$$0 \leq q_k \leq p_k \leq \nu_k \tag{24}$$

The criteria difference for each pair of alternatives [i,j] and each criterion k is known:

$$\Delta_k[i, j] = \alpha_k(f_k(i) - f_k(j)) \tag{25}$$

for i =1, . . . , m, j = 1, . . . , m, j ≠ i, k = 1, . . . , n, and where α_k is an optimization indicator ($\alpha_k = 1$ if f_k is to be maximized and $\alpha_k = -1$ if f_k is to be minimized). A global concordance index $C[i,j]$ is then calculated as with ELECTRE III for each pair of alternatives (for i = 1, . . . , m and j = 1 , . . . , m)[28]:

TABLE IV
Kinetic Parameters Identified for the Polymerization of Styrene at 60°C

Parameters	Significance	Value
f	Initiator efficiency	0.5
k_d	Initiator dissociation rate constant	7.35×10^{-6} s^{-1}
k_p	Propagation rate constant	354 L/mol s
k_{trM}	Transfer to monomer rate constant	9.35×10^{-3} L/mol s
k_{cm}	Nucleation rate constant	7.85×10^{-5} L/g s
k_{cp}	Capture rate constant	5.56×10^{-14} L/mol m s
S_e	Limited concentration of surfactant	0.514 g/L
a_s	Surface area occupied by 1 g of surfactant	1.91×10^5 dm^2/g

$$C[i,j] = \sum_{k=1}^{n} w_k \cdot c_k[i,j] \text{ where}$$

$$c_k[i,j] = \begin{cases} 1 & \text{if } -\Delta_k[i,j] \le q_k \\ \dfrac{\Delta_k[i,j] + p_k}{p_k - q_k} & \text{if } q_k < -\Delta_k[i,j] \le p_k \\ 0 & \text{if } p_k < -\Delta_k[i,j] \end{cases} \quad (26)$$

The preference of a point vs another is said concordant up to the indifference threshold and the local concordance index is then equal to 1. On the contrary, it is said not concordant up to the preference threshold and the local concordance index is then equal to 0. Between these two thresholds, a linear approach is used to define the local concordance index.

A discordance index $D_k[i,j]$ is also calculated for each criterion k as with ELECTRE III, to take into account a bad criterion value, which allows to relegate the concerned point in the total ranking (for $i = 1, \ldots, m$, $j = 1, \ldots, m$, and $k = 1, \ldots, n$)[28]:

$$D_k[i,j] = \begin{cases} 0 & \text{if } -\Delta_k[i,j] \le p_k \\ \dfrac{-\Delta_k[i,j] - p_k}{\nu_k - p_k} & \text{if } p_k < -\Delta_k[i,j] \le \nu_k \\ 1 & \text{if } \nu_k < -\Delta_k[i,j] \end{cases} \quad (27)$$

The preference of a point vs another is said discordant up to the veto threshold and the discordance index is then equal to 1. On the contrary, it is said not discordant up to the preference threshold and the discordance index is then equal to 0. Between these two thresholds, a linear approach is used to define the discordance index.

Using the concordance and the discordance indexes, outranking degrees $\sigma[i,j]$ are generated for every pair of alternatives. These outranking degrees are obtained using the following formula (for$i = 1, \ldots, m$ and $j = 1, \ldots, m$)[29]:

$$\sigma[i,j] = C[i,j] \cdot \prod_{k=1}^{n} [1 - (D_k[i,j])^3] \quad (28)$$

The i outranks j all the more than the outranking degree is close to 1 ($0 \le \sigma[i,j] \le 1$). The resulting outranking relation sets may be represented as an outranking matrix. From these outranking degrees, two preorders are established as with PROMETHEE by the outgoing flow σ_i^+ and the incoming flow σ_i^- (for $i = 1, \ldots, m$)[30]:

$$\sigma_i^+ = \sum_{j=1}^{m} \sigma[i,j] \quad \text{and} \quad \sigma_i^- = \sum_{j=1}^{m} \sigma[j,i] \quad (29)$$

Finally, the total ranking of the alternatives i is determined from the net flow with possible *ex æquo* (for $i = 1, \ldots, m$):

$$\sigma_i = \sigma_i^+ - \sigma_i^- \quad (30)$$

The alternative that has the highest net flow is considered the best solution, and the one that has the lowest net flow is considered the worst solution, also called "nadir."

RESULTS AND DISCUSSION

Identification of the model parameters

The parameters were determined from experimental data. The aim is to minimize the difference between experimental and simulated values. The available experimental data are the conversion, the particles number, and the number and weight average molecular weights.[31,32] So, a maximum likelihood criterion was used to take into account the scale problem of the measures. This criterion is given, for the same number of data of each measure, by[33]

$$J = \ln\left(\sum_{\text{data}} (X_{\text{exp}} - X_{\text{sim}})^2\right) + \ln\left(\sum_{\text{data}} (N_{p\text{exp}} - N_{p\text{sim}})^2\right) + \ln\left(\sum_{\text{data}} (\bar{M}_{n\text{exp}} - \bar{M}_{n\text{sim}})^2\right) + \ln\left(\sum_{\text{data}} (\bar{M}_{w\text{exp}} - \bar{M}_{w\text{sim}})^2\right) \quad (31)$$

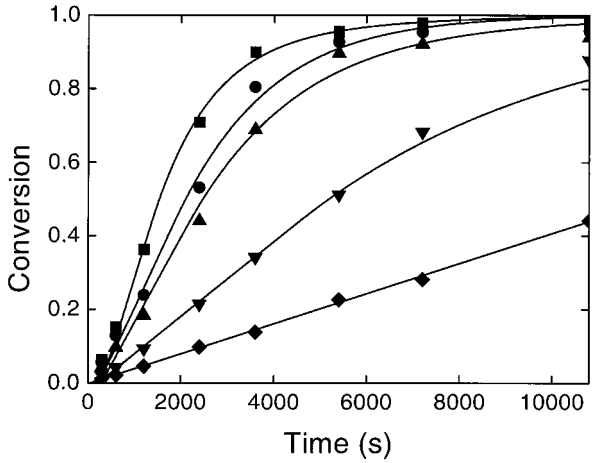

Figure 2 Comparison between simulated and experimental conversions. $I_0 = 3.7 \times 10^{-3}$ mol/L. Influence of the initial concentration of the surfactant: $S_0 = 0.31$ CMC (◆); $S_0 = 0.53$ CMC (▼); $S_0 = 1.06$ CMC (▲); $S_0 = 1.60$ CMC (●); $S_0 = 2.13$ CMC (■); simulation (—).

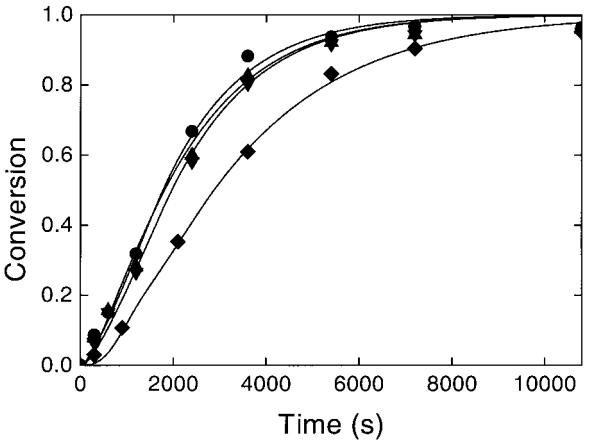

Figure 3 Comparison between simulated and experimental conversions. $S_0 = 2.13$ CMC. Influence of the initial concentration of the initiator: $I_0 = 0.92 \times 10^{-3}$ mol/L (◆); $I_0 = 1.85 \times 10^{-3}$ mol/L (▼); $I_0 = 2.22 \times 10^{-3}$ mol/L (▲); $I_0 = 2.96 \times 10^{-3}$ mol/L (●); simulations (—).

Table IV presents the kinetic parameters estimated for the styrene polymerization. The initiator efficiency was found to be equal to 0.5. The initiator dissociation rate constant for potassium persulfate is comparable to these found in the literature at 60°C: 5.3×10^{-6} s^{-1} or 4.6×10^{-6} s^{-1}.[9,34] The propagation rate constant is of the same order of magnitude in the literature, 345 L/mol s or 105 to 376 L/mol s.[9,11] The transfer to monomer rate constant, generally about 10^{-2} L/mol s at 60°C, is consistent with the obtained value.[35] The other parameters are specific for our model.

Validation of the model for different experimental conditions

Monomer conversion

Figures 2 and 3 compare experimental and simulated values of the conversion for several experiments. The effect of initial concentrations of surfactant and initiator are well illustrated: the polymerization rate decreases as these concentrations decrease. Moreover, the model remains satisfactory for concentrations lower than the CMC.

Number of particles

Experimental and simulated number of particles are presented in Figures 4 and 5. Again, the effect of the initial concentration of surfactant is very well simulated, above and below the CMC. This means that homogeneous and micellar nucleations are correctly taken into account in the model.

Number and weight average molecular weights

Figures 6 and 7 show the experimental and simulated evolutions of the number average molecular weights, while Figures 8 and 9 represent the weight average molecular weights. We can notice that the simulated values tends to underestimate the experimental $\bar{M}_n$ values above 10^6 g/mol. Nevertheless, the simulation represents these physical tendencies very well.

Average number of radicals per particle

Finally, the average number of radicals per particle is shown in Figure 10, which verifies the assumption of the zero-one model ($\bar{n} \sim 0.5$). This simulation is valid whatever the initial conditions.

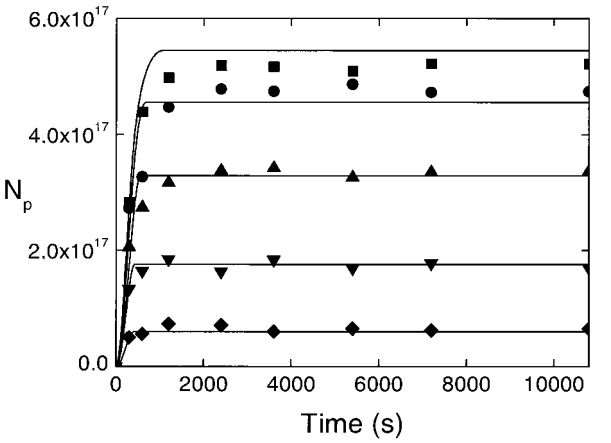

Figure 4 Comparison between simulated and experimental particles number. $I_0 = 3.7 \times 10^{-3}$ mol/L. Influence of the initial concentration of the surfactant: $S_0 = 0.31$ CMC (◆); $S_0 = 0.53$ CMC (▼); $S_0 = 1.06$ CMC (▲); $S_0 = 1.60$ CMC (●); $S_0 = 2.13$ CMC (■); simulation (—).

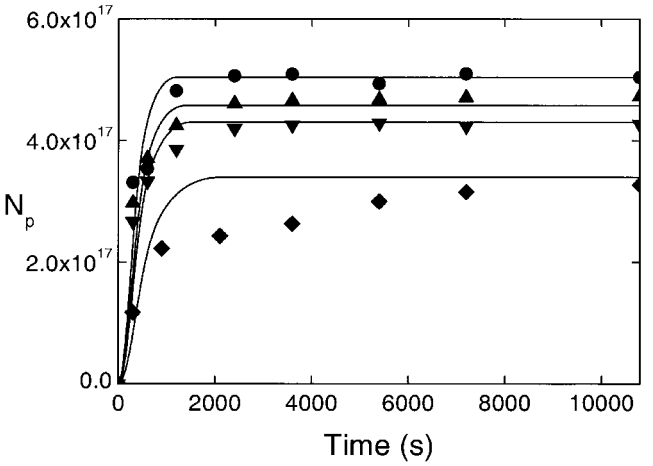

Figure 5 Comparison between simulated and experimental particles number. S_0 = 2.13 CMC. Influence of the initial concentration of the initiator: $I_0 = 0.92 \times 10^{-3}$ mol/L (◇); $I_0 = 1.85 \times 10^{-3}$ mol/L (▼); $I_0 = 2.22 \times 10^{-3}$ mol/L (▲); $I_0 = 2.96 \times 10^{-3}$ mol/L (●); simulations (—).

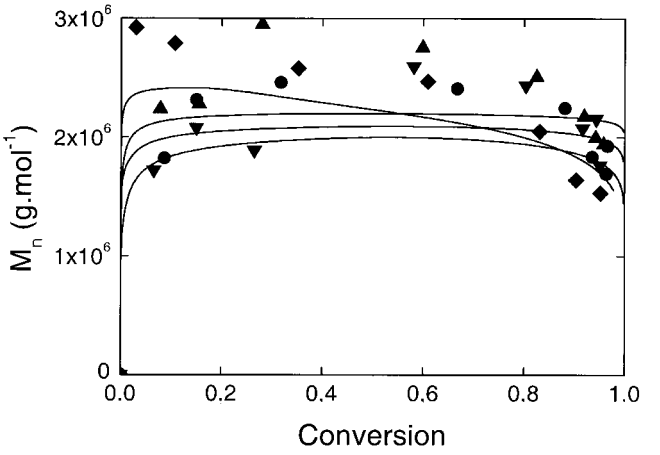

Figure 7 Comparison between simulated and experimental number average molecular weights. S_0 = 2.13 CMC. Influence of the initial concentration of the initiator: $I_0 = 0.92 \times 10^{-3}$ mol/L (◆); $I_0 = 1.85 \times 10^{-3}$ mol/L (▼); $I_0 = 2.22 \times 10^{-3}$ mol/L (▲); $I_0 = 2.96 \times 10^{-3}$ mol/L (●); simulations (—).

Multicriteria optimization

The elaborated model allows us to obtain the conversion, the number of particles per liter, the number and weight average molecular weights for different initial experimental conditions, i.e., initial concentrations of initiator, monomer, and surfactants, for a given time of polymerization, t_f. So, inputs, which are used as decision variables in multiobjective optimization, and outputs of the simulation model are defined.

From the outputs, a production criterion, f_1, to be maximized, is defined by

$$f_1 = X(t_f) \tag{32}$$

Two "quality" criteria, f_2 and f_3, are also defined:

$$f_2 = |N_p(t_f) - N_{pd}| \tag{33}$$

$$f_3 = |\bar{M}_w(t_f) - \bar{M}_{wd}| \tag{34}$$

where N_{pd} and $\bar{M}_{wd}$ denote the desired values of the number of particles and the weight average molecular weight. The objective is to minimize these two criteria in order to approach the desired values. In this problem, the final time of polymerization and the initial concentration of monomer are fixed. The aim is to determine initial concentrations of initiator and surfactant such as the three criteria, f_1, f_2, and f_3 are simultaneously optimized.

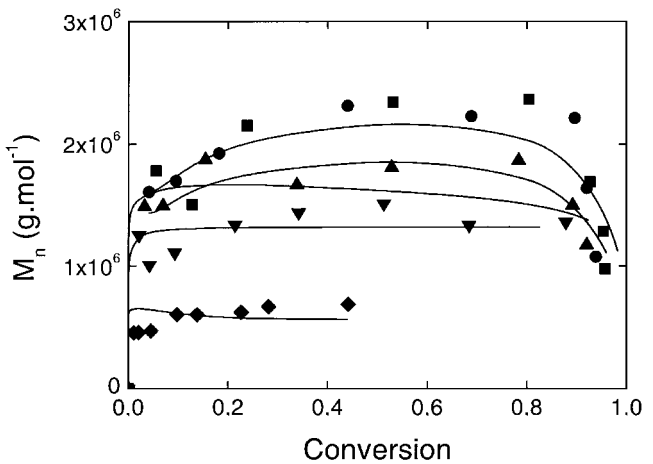

Figure 6 Comparison between simulated and experimental number average molecular weights. $I_0 = 3.7 \times 10^{-3}$ mol/L. Influence of the initial concentration of the surfactant: S_0 = 0.31 CMC (◆); S_0 = 0.53 CMC (▼); S_0 = 1.06 CMC (▲); S_0 = 1.60 CMC (●); S_0 = 2.13 CMC (■); simulation (—).

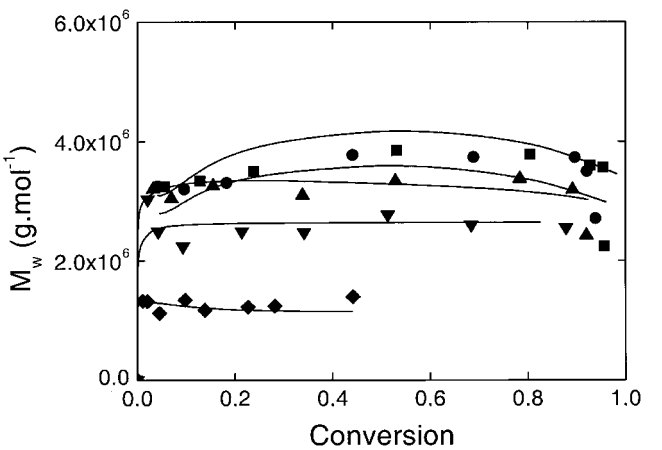

Figure 8 Comparison between simulated and experimental weight average molecular weights. $I_0 = 3.7 \times 10^{-3}$ mol/L. Influence of the initial concentration of the surfactant: S_0 = 0.31 CMC (◆); S_0 = 0.53 CMC (▼); S_0 = 1.06 CMC (▲); S_0 = 1.60 CMC (●); S_0 = 2.13 CMC (■); simulation (—).

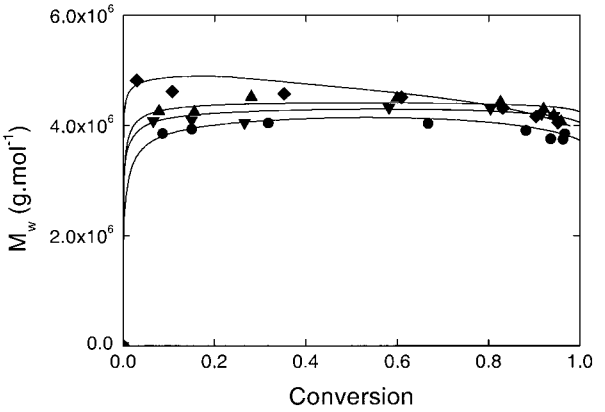

Figure 9 Comparison between simulated and experimental weight average molecular weights. S_0 = 2.13 CMC. Influence of the initial concentration of the initiator: $I_0 = 0.92 \times 10^{-3}$ mol/L (◆); $I_0 = 1.85 \times 10^{-3}$ mol/L (▼); $I_0 = 2.22 \times 10^{-3}$ mol/L (▲); $I_0 = 2.96 \times 10^{-3}$ mol/L (●); simulations (—).

The simulation package is coupled with the optimization loop for performing the multiobjective optimization. Using the principle of the evolutionary algorithm, random input vectors are proposed for initialization before entering the optimization loop. From these vectors, composed of $[I]_0$, $[M]_0$, S_0, and t_f, the simulation model is able to predict output values of $X(t)$, $N_p(t)$, $\bar{M}_n(t)$, and $\bar{M}_w(t)$. The three criteria, f_1, f_2, and f_3, are so deduced, and the domination function F is calculated for each input vector. The optimization loop is done until all input vectors have been nondominated.

The following two desired values define the quality criteria:

$$N_{pd} = 5 \times 10^{17} \text{ part/l} \tag{35}$$

$$\bar{M}_{wd} = 2.5 \times 10^6 \text{ g/mol} \tag{36}$$

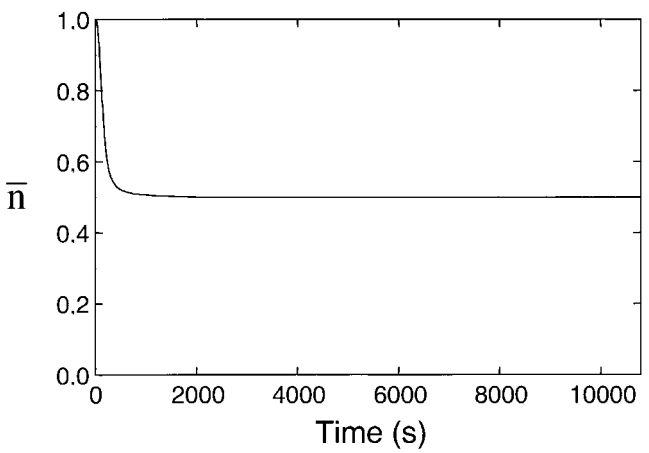

Figure 10 Simulation of the average number of free radicals per particle.

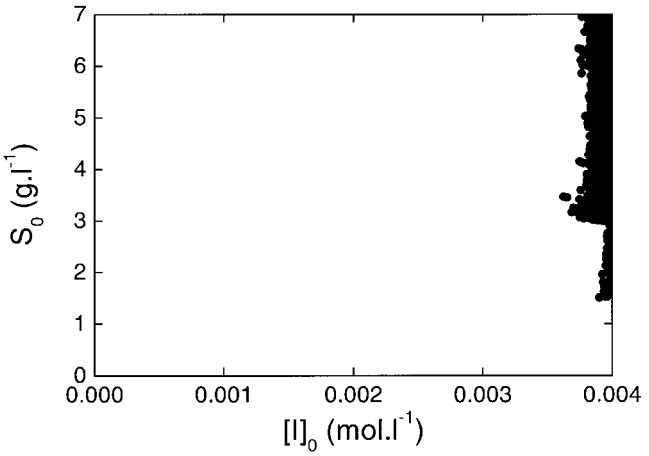

Figure 11 Pareto zone for initial concentrations of initiator and surfactant.

Moreover, constant values for the given recipe, and the search space of the inputs, are defined:

$$[M]_0 = 2.184 \text{ mol/l} \tag{37}$$

$$t_f = 10800 \text{ s} \tag{38}$$

$$0 \leq [I]_0 \leq 4 \times 10^{-3} \text{ mol/l} \tag{39}$$

$$0 \leq S_0 \leq 7 \text{ g/l} \tag{40}$$

Figure 11 shows the resulting Pareto zone formed with 5000 points and obtained for the inputs $[I]_0$ and S_0. We can notice that this zone is located on the upper border of the space of the initial concentration of initiator. So, the three criteria can be simultaneously optimized with a precise concentration of initiator (most values between 3.8×10^{-3} and 4×10^{-3} mol/L) and a range surfactant concentration (values between 1.5 and 7 g/L). This first bit of information allows us to know which initial conditions can be used, to reach the desired characteristics of the latex.

Interesting information is also given by the Pareto front represented in Figure 12. The three dimensions are represented by projection of one criterion over the two others. The Pareto front is a surface in a three dimensional space. We can notice the form of this front, due to the criteria in absolute values. Figure 12(a) shows that the desired value of the number of particles is reached with a conversion about 95%. For higher conversions, other values of N_p are determined. On the other hand, in Figure 12(b), the desired values for N_p and $\bar{M}_w$ are never obtained in the same time ($N_p = 5 \times 10^{17}$ for $|\bar{M}_w(\text{tf}) - \bar{M}_{wd}| \approx 8 \times 10^5$ g/mol and $\bar{M}_w$ 2.5 $\times 10^6$ g/mol for $|N_p(t_f) - N_{\text{pd}}| \approx 1.5 \times 10^{17}$). The ideal solution, at the origin, does not exist. Again, the two criteria represented on Figure 12(c) are in

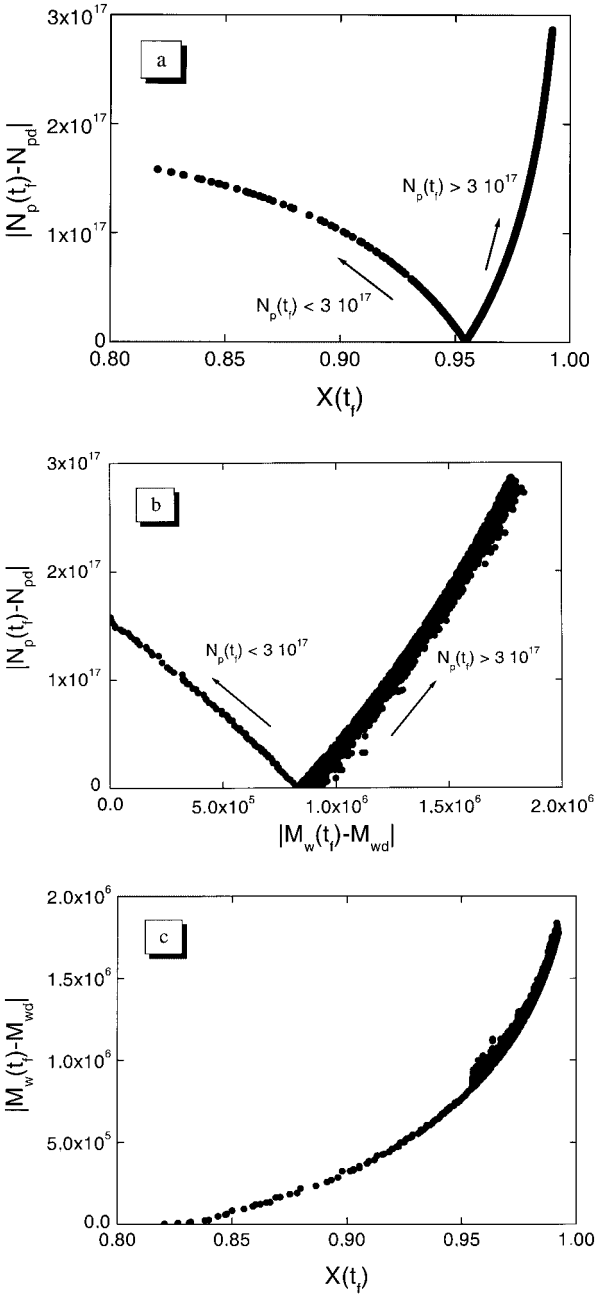

Figure 12 Pareto front for the three criteria. (a) f_2 vs f_1; (b) f_2 vs f_3; (c) f_3 vs f_1.

conflict. The more the conversion is high, the less the desired value of weight average molecular weight is reached.

TABLE V
Weights and Thresholds Definition for the Net Flow Algorithm

	w_k	q_k	p_k	v_k
f_1 (production)	1/3	0.01	0.03	0.05
f_2 (quality N_p)	1/3	5×10^{14}	5×10^{15}	5×10^{16}
f_3 (quality M_w)	1/3	10^4	10^5	5×10^5

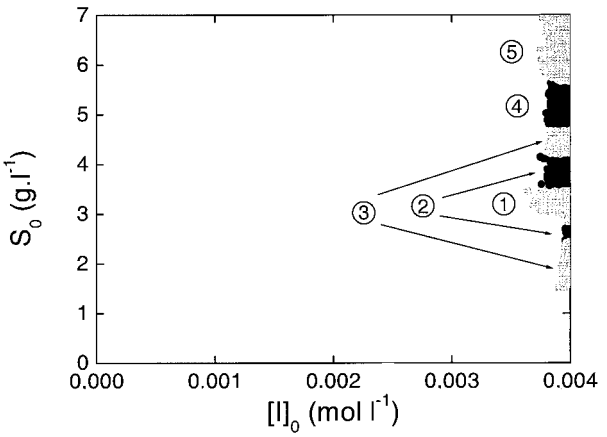

Figure 13 Quintiles of the Pareto zone obtained by the decision support system, for initial concentrations of initiator and surfactant.

The results of the multicriteria optimization allowed us to eliminate a lot of solutions that are not interesting for our problem. The zone of interest has been kept after the introduction of the nondomination concept. Preferences have now to be introduced to get the best trade-off.

Decision aid

From the nondominated solutions obtained, a decision support system is able to propose a trade-off solution. The results depend on the choice of the preferences given by a human being. Weights and thresholds have to be chosen for all three criteria. These preferences are presented in Table V and result from the choice of an expert.

A total ranking is generated from the definition of these preferences. Figure 13 presents the results in quintiles, which are classified subsets of the Pareto zone. The first quintile, i.e., the first 1000 points, is the most interesting subset and the characteristics of the best trade-off obtained by the decision aid algorithm are presented in Table VI. This best solution is located in the center of the first subset.

The corresponding subsets in the Pareto front are represented in Figure 14. The best solution is situated in the center of the Pareto front and nearly corre-

TABLE VI
Characteristics of the Best Point Obtained by the Net Flow Algorithm

	Best solution
$[I]_0$ (mol/L)	3.99×10^{-3}
S_0 (g/L)	2.99
$X(t_f)$	0.955
$\lvert N_p(t_f) - N_{pd}\rvert$	1.1×10^{15}
$\lvert M_w(t_f) - M_{wd}\rvert$ (g/mol)	8.34×10^5

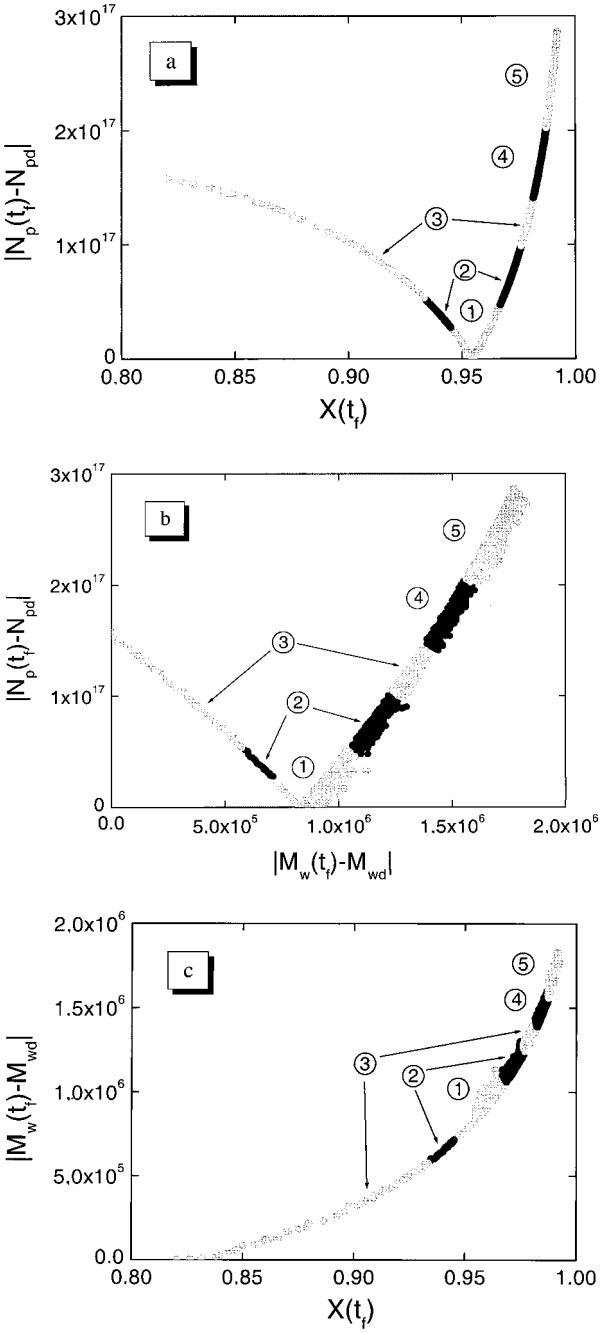

Figure 14 Quintiles of the Pareto front, obtained by the decision support system, for the three criteria. (a) f_2 vs f_1; (b) f_2 vs f_3; (c) f_3 vs f_1.

sponds to the optimal number of particles. This solution has a rather satisfied weight average molecular weight and a good conversion. So, this solution is considered as the best trade-off of this problem.

The best solution, considered as the best trade-off, is obtained from the preferences of the decision maker. It is a subjectivity part, introduced in a second step, after the determination of a set of non dominated solutions. So, the result is sensitive to the definition of the weights and thresholds.

CONCLUSION

In this study, a new methodology has been developed to solve multicriteria decision problems and has been applied to the emulsion polymerization of styrene. This approach has taken into account the elaboration of a kinetic model, followed by the development of optimization and decision procedures. For this process, we have chosen operating and initial conditions that allowed us to obtain a final product with desired qualities and to optimize the production. The aim has been to simultaneously optimize several conflicting criteria. The decision aid has contributed to improve the multicriteria optimization approach.

The simulation model is able to describe some characteristics of both macromolecules and latex particles. This model was elaborated from knowledge of physicochemical phenomena. It used a kinetic scheme with the corresponding population balances and adopted a zero-one concept to correctly predict the conversion, the number of particles, and the number and weight average molecular weights of the resulting macromolecules. This simulation tool has been elaborated to be used in a multicriteria optimization procedure. Two other steps have been necessary to develop completely the methodology. The first one has allowed to determine a zone of interest without *a priori* using the domination concept. The second one has allowed us to chose the best trade-off from preferences defined by a decision maker. Finally, in this example (emulsion polymerization of styrene), the multicriteria optimization has provided interesting information for the initial concentration of initiator while the decision aid has proposed one for the initial concentration of surfactant.

This methodological approach has been applied to a simple zero-one model, but it may be necessary to optimize required customer properties. Depending on the application (e.g. , paints or adhesives), the simultaneous optimization of several properties (e.g., film forming, scrub resistance, adhesion) will be interesting.

References

1. Pareto, V. Cours d'économie politique; F. Rouge: Lausanne, 1896.
2. Bhaskar, V.; Gupta, S. K.; Ray, A. K. Rev Chem Eng 2000, 16, 1, 1.
3. Mitra, K.; Deb, K.; Gupta, S. K. J Appl Polym Sci 1998, 69, 69.
4. Garg, S.; Gupta, S. K. Macromol Theory Simul 1999, 8, 1, 46.
5. Bhaskar, V.; Gupta, S. K.; Ray, A. K. AIChE J 2000, 46, 1046.
6. Zhou, F.; Gupta, S. K.; Ray, A. K. J Appl Polym Sci 2000, 78, 1439.
7. Mankar, R. B.; Saraf, D. N.; Gupta, S. K. J Polym Eng 1998, 18, 371.
8. Garg, S.; Gupta, S. K.; Saraf, D. N. J Appl Polym Sci 1999, 71, 2101.
9. Gilbert, R. G. Emulsion Polymerization. A Mechanistic Approach; Academic Press: San Diego, CA, 1995.

10. Asua, J. M.; Adams, M. E.; Sudol, E. D. J Appl Polym Sci 1990, 39, 1183.
11. Bataille, P.; Van, V. T.; Pham, Q. B. J Polym Sci, Polym Chem Ed 1982, 20, 795.
12. Harkins, W. D. J Am Chem Soc 1947, 69, 1428.
13. Smith, W. V.; Ewart, R. H. J Chem Phys 1948, 16, 6, 592.
14. Gardon, J. L. J Polym Sci. : Part. A1 1968, 6, 623.
15. Fitch, R. M.; Tsai, C. H. Polym Lett 1970, 8, 703.
16. Hansen, F. K.; Ugelstad, J. J Polym Sci, Polym Chem Ed 1978, 16, 1953.
17. Lichti, G.; Gilbert, R. G.; Napper, D. H. J Polym Sci, Polym Chem Ed 1983, 21, 269.
18. Chern, C. S.; Lin, C. H. Polymer 1998, 40, 139.
19. Hansen, F. K.; Ugelstad, J. J Polym Sci., Polym. Chem. Ed 1979, 17, 3069.
20. Fitch, R. M.; Tsai, C. H. In Polymer Colloids; Fitch, R. M., Ed.; Plenum: New York, 1971; Chap 3.
21. Nomura, M.; Horie, I.; Kubo, M.; Fujita, K. J Appl Polym Sci 1989, 37, 1029.
22. Villermaux, J.; Blavier, L. Chem Eng Sci 1984, 39, 1, 87.
23. Oliveira, A. T. M.; Biscaia, E. C.; Pinto, J. C. J Appl Polym Sci 1998, 69, 1137.
24. Fonseca, C. M.; Fleming, P. J. Evolutionary Computation 1995, 3, 16.
25. Fonteix, C.; Bicking, F.; Perrin, E.; Marc, I. Int J Syst Sci 1995, 26, 10, 1919.
26. Perrin, E.; Mandrille, A.; Oumoun, M.; Fonteix, C.; Marc, I. RAIRO—Recherche Opérationnelle 1997, 31, 2, 161.
27. Roy, B.; Bouyssou, D. Aide multicritère à la décision: méthodes et cas; Economica: Paris, 1993.
28. Roy, B. Cahier du CERO 1978, 20, 1, 3.
29. Rousseau, A.; Martel, J. M. In Applying Multiple Criteria Aid for Decision to Environmental Management; Paruccini M. Ed.; Kluwer Academic: New York, 1994; p 163.
30. Brans, J. P.; Vincke, P. Management Science 1985, 31, 6, 647.
31. Castellanos Ortega, J. R. Ph.D. thesis, INPL, 1996.
32. Massebeuf, S. Ph.D. thesis, INPL, 2000.
33. Walter, E.; Pronzato, L. Identification of Parametric Models from Experimental Data; Springer: London, 1997.
34. Brandrup, J.; Immergut, E. H. In Polymer Handbook, 3rd ed.; Wiley Interscience: New York, 1989.
35. Gentric, C.; Pla, F.; Latifi, M. A.; Corriou, J. P. Chem Eng J 1999, 75, 31.